

# Reduced methane growth rate explained by decreased Northern Hemisphere microbial sources

Fuu Ming Kai<sup>1†</sup>, Stanley C. Tyler<sup>1†</sup>, James T. Randerson<sup>1</sup> & Donald R. Blake<sup>2</sup>

Atmospheric methane ( $\text{CH}_4$ ) increased through much of the twentieth century, but this trend gradually weakened until a stable state was temporarily reached around the turn of the millennium<sup>1,2</sup>, after which levels increased once more<sup>3</sup>. The reasons for the slowdown are incompletely understood, with past work identifying changes in fossil fuel, wetland and agricultural sources and hydroxyl (OH) sinks as important causal factors<sup>1,4–8</sup>. Here we show that the late-twentieth-century changes in the  $\text{CH}_4$  growth rates are best explained by reduced microbial sources in the Northern Hemisphere. Our results, based on synchronous time series of atmospheric  $\text{CH}_4$  mixing and  $^{13}\text{C}/^{12}\text{C}$  ratios and a two-box atmospheric model, indicate that the evolution of the mixing ratio requires no significant change in Southern Hemisphere sources between 1984 and 2005. Observed changes in the interhemispheric difference of  $^{13}\text{C}$  effectively exclude reduced fossil fuel emissions as the primary cause of the slowdown. The  $^{13}\text{C}$  observations are consistent with long-term reductions in agricultural emissions or another microbial source within the Northern Hemisphere. Approximately half ( $51 \pm 18\%$ ) of the decrease in Northern Hemisphere  $\text{CH}_4$  emissions can be explained by reduced emissions from rice agriculture in Asia over the past three decades associated with increases in fertilizer application<sup>9</sup> and reductions in water use<sup>10,11</sup>.

Several mechanisms have been proposed to explain the long-term slowdown of atmospheric  $\text{CH}_4$ , including decreases in source emissions<sup>4,5,8,10,12</sup>, changes in sink processes<sup>7</sup>, and a stabilization of  $\text{CH}_4$  with relatively constant global emissions<sup>1</sup>. Using a three-dimensional atmospheric model, Bousquet *et al.*<sup>5</sup> provide evidence from a Bayesian inversion that the  $\text{CH}_4$  slowdown in the 1990s was caused partly by decreases in fossil emissions in the Northern Hemisphere. Carbon and hydrogen isotope measurements have become an important means of determining the magnitude of sources and sinks of atmospheric  $\text{CH}_4$  (ref. 13), including assessments of interannual- to centennial-scale trends in the global budget<sup>5,14–16</sup>. Here we analysed isotope and mixing ratio measurements from the University of California, Irvine (UCI), National Institute of Water and Atmospheric Research (NIWA) and the University of Washington, Stable Isotope Laboratory (SIL) networks<sup>2,15–17</sup> (Supplementary Table 1). Our goal was to quantify inter-hemispheric differences (IHDs) of  $\text{CH}_4$ ,  $\delta^{13}\text{C}-\text{CH}_4$  and  $\delta\text{D}-\text{CH}_4$ , and to assess how they constrain recent changes in the global  $\text{CH}_4$  budget.

From the mixing ratio measurements, we could see that  $\text{CH}_4$  growth rates in both hemispheres declined during 1979–2005 (Supplementary Fig. 1). The IHD of  $\text{CH}_4$  (defined as Northern Hemisphere  $\text{CH}_4$  minus Southern Hemisphere  $\text{CH}_4$ ) started at approximately  $80 \pm 20$  parts per billion (p.p.b.) during 1979–1981, and gradually increased to

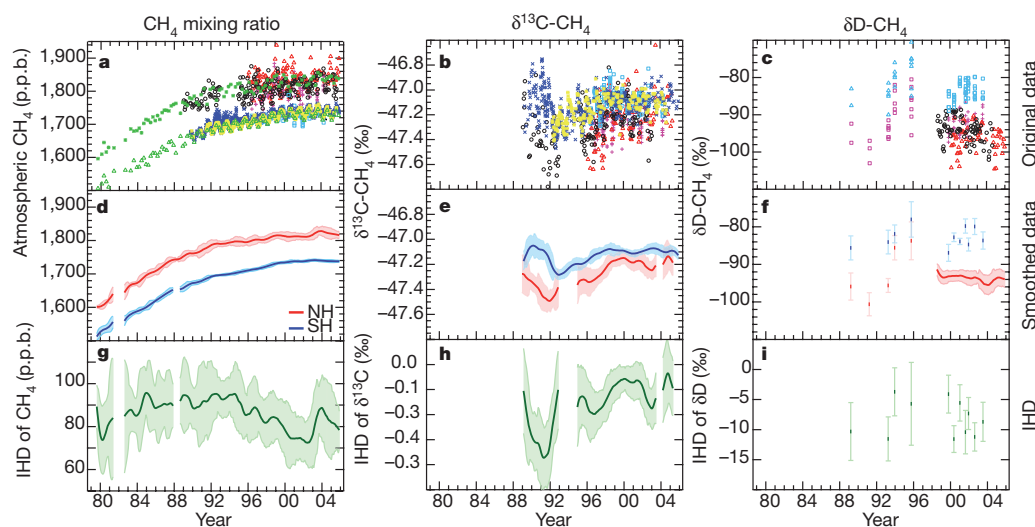


**Figure 1 | Long-term trends in atmospheric  $\text{CH}_4$ ,  $\delta^{13}\text{C}-\text{CH}_4$ , and  $\delta\text{D}-\text{CH}_4$ .** The left panels show  $\text{CH}_4$ ; the middle panels show  $\delta^{13}\text{C}-\text{CH}_4$  and the right panels show  $\delta\text{D}-\text{CH}_4$ . **a–c**, Original measurements used to construct the Northern Hemisphere and Southern Hemisphere time series. The observing stations are Niwot Ridge (black circles), Montana de Oro (red triangles), the Pacific Ocean cruise in the Northern Hemisphere (POCNH; magenta pluses), the UCI network  $40^\circ\text{N}$  (green asterisks), the SIL-POCNH (magenta squares), Baring Head (blue crosses), Scott Base (yellow asterisks), the Pacific Ocean cruise in the Southern Hemisphere (POCSH; cyan squares), the UCI network

$40^\circ\text{S}$  (green triangles), and the SIL-POCSH (cyan triangles). **d–f**, Twelve-month smoothed trends in the Northern Hemisphere (red line) and Southern Hemisphere (blue line). The smoothed trends were constructed after removing an annual cycle and applying an offset to each station based on hemisphere-specific reference sites. **g–i**, IHDs (green lines) were defined as the difference between the Northern Hemisphere and Southern Hemisphere smoothed time series in **d** to **f**. Error bars are one standard deviation (s.d.), on the basis of all the adjusted observations in a 12-month window centred at each monthly time step. For  $\delta\text{D}-\text{CH}_4$ , the error bars are one s.d. of the Pacific voyage measurements.

<sup>1</sup>Department of Earth System Science, University of California, Irvine, California 92697, USA. <sup>2</sup>Department of Chemistry, University of California, Irvine, California 92697, USA. <sup>†</sup>Present addresses: Singapore-MIT Alliance for Research and Technology, S16-05-08, 3 Science Drive 2, 117543 Singapore (F.M.K.); Department of Chemistry, Norco College, Norco, California 92860, USA (S.C.T.).

93 ± 11 p.p.b. during 1991–1995 (Fig. 1). The IHD subsequently decreased from 1995 to 2002, reaching a mean of 79 ± 10 p.p.b. during 2001–2005. For  $\delta^{13}\text{C}$ , the Southern Hemisphere measurements indicated no significant long-term trend, with the mean during 1989–1993 ( $-47.16 \pm 0.09\text{‰}$ ; mean ± standard deviation, s.d.) almost the same as the mean during 2001–2005 ( $-47.09 \pm 0.01\text{‰}$ ). In contrast,  $\delta^{13}\text{C}$  in the Northern Hemisphere increased from  $-47.40 \pm 0.07\text{‰}$  to  $-47.19 \pm 0.03\text{‰}$  (Fig. 1e). As a result, the IHD of  $\delta^{13}\text{C}$  narrowed from  $-0.24 \pm 0.11\text{‰}$  to  $-0.10 \pm 0.04\text{‰}$  over this time period (Fig. 1h). Considered separately from other constraints, the trend towards relatively enriched carbon isotope values in the Northern Hemisphere implied (1) a decrease in sources with isotopically depleted signatures (for example, agriculture, landfills or wetlands), (2) an increase in sources that were isotopically enriched (for example, Northern Hemisphere fossil fuel emissions or biomass burning), or (3) an increase in atmospheric removal by reaction with hydroxyl radical (OH) in the Northern Hemisphere.

We also found that  $\delta\text{D}-\text{CH}_4$  did not change substantially in the Northern Hemisphere during 1989–2005 (Fig. 1f). Northern Hemisphere  $\delta\text{D}$  remained nearly at  $-94 \pm 1\text{‰}$  between 1998 and 2005. The IHD of  $\delta\text{D}-\text{CH}_4$  ranged from  $-12.5$  to  $-2.5\text{‰}$  during the cruises made by the SIL network between 1989 and 1996 (Fig. 1i). Because of the sensitivity of  $\delta\text{D}-\text{CH}_4$  to sink processes<sup>15</sup>, the relatively constant  $\delta\text{D}-\text{CH}_4$  suggested that there was not a substantial long-term change in the OH sink between 1998 and 2005. Other factors potentially influence  $\delta\text{D}-\text{CH}_4$ , however, and so to estimate quantitatively the impacts of possible changes in the OH sink<sup>7</sup>, we conducted several sensitivity simulations (Supplementary Table 2).

To assess the implications of the measurements described above and to examine recent competitive hypotheses related to the levelling off of  $\text{CH}_4$  mixing ratios, we constructed global  $\text{CH}_4$  budget scenarios using a two-box atmospheric model<sup>18</sup> (see Supplementary Methods). In a first step, we constructed a control simulation (scenario 1) that included natural and anthropogenic  $\text{CH}_4$  sources (Supplementary Fig. 2). In this simulation, anthropogenic emissions associated with fossil fuels and agriculture—two of the largest anthropogenic terms—remained constant after 1980 (Supplementary Fig. 2a and b). We compared model estimates of  $\text{CH}_4$  mixing and isotope ratio with observations, which were extended back in time with firn air and ice core measurements of  $\text{CH}_4$  (ref. 19) and  $\delta^{13}\text{C}-\text{CH}_4$  (ref. 20). The control captured the long-term trends in  $\text{CH}_4$  and most of the variations in the  $\text{CH}_4$  IHD (Supplementary Fig. 2c and d). Considering  $\text{CH}_4$  changes alone, these results appear to suggest that the long-term  $\text{CH}_4$  slowdown can be explained by the levelling off of both fossil and agricultural emissions. However, differences between the model estimates and observations of  $\delta^{13}\text{C}-\text{CH}_4$  were substantial. For example, the model IHD of  $\delta^{13}\text{C}-\text{CH}_4$  remained approximately the same during 1989–2005, whereas the observations showed an increasing trend (a lessening of the IHD (Supplementary Fig. 2f). The differences between the observed and modelled IHD in  $\delta^{13}\text{C}-\text{CH}_4$  implied that agricultural and fossil emissions may have had diverging trajectories and provided motivation for exploring the different emissions scenarios described below.

In past work, decreases in fossil fuel emissions have been implicated as an important driver of the methane slowdown<sup>5,8,12</sup>. To assess this hypothesis using our isotope data, we constructed a second scenario assuming that fossil fuel emissions were solely responsible for the observed  $\text{CH}_4$  trends and assuming that all the other sources were the same as in the control. First, we estimated the total flux of  $\text{CH}_4$  in the two hemispheres using the smoothed observations (Fig. 1d) and a simple mass-balance inversion during 1984–2005. Figure 2a shows that the Northern Hemisphere flux decreased from  $417 \pm 10 \text{ Tg CH}_4 \text{ yr}^{-1}$  during 1984–1985 to  $386 \pm 5 \text{ Tg CH}_4 \text{ yr}^{-1}$  during 2004–2005. In parallel, the Southern Hemisphere flux showed no significant change, starting at  $148 \pm 5$  and ending at  $150 \pm 5 \text{ Tg CH}_4 \text{ yr}^{-1}$  during this period.

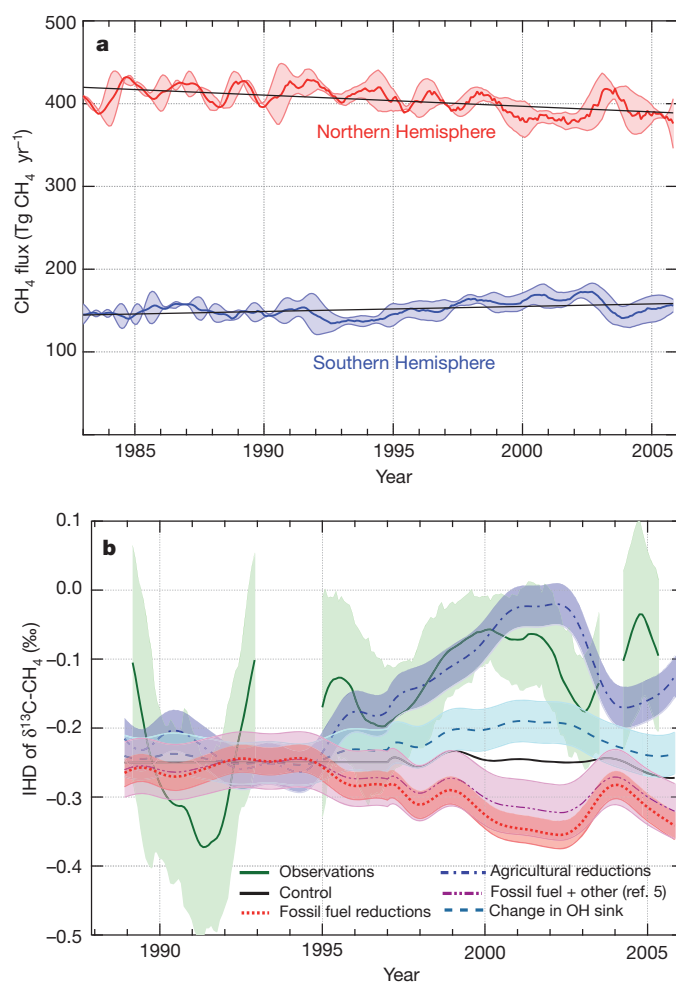


**Figure 2 | Variations in  $\text{CH}_4$  fluxes and the impacts of source composition on isotopic trends.** **a**, The  $\text{CH}_4$  fluxes in both hemispheres were obtained from a mass-balance inversion using the mixing ratio observations shown in Fig. 1d. **b**, Comparison of the observed IHD of  $\delta^{13}\text{C}$  with model scenarios during 1989–2005. The simulation with decreases in fossil fuel emissions (scenario 2) did not capture the trend in the observed IHD of  $\delta^{13}\text{C}$ : the  $\delta^{13}\text{C}$  IHD in this scenario widened over 1989–2005. In contrast, the simulation with decreases in agricultural emissions (scenario 3) had an increasing trend in the IHD of  $\delta^{13}\text{C}$ , similar to the observations. A scenario that included decreases in fossil fuels and other sources from ref. 5 (scenario 4) had a negative slope that fell between the control and fossil fuel scenarios. Additional sensitivity simulations with changes in sink processes (scenario 7 as described in the Supplementary Information) show the maximum potential for OH variability to contribute to the observed trend. For the  $\text{CH}_4$  fluxes, error bars are one s.d. estimates of the fluxes derived from our inversion in a 12-month window centred at each monthly time step. For comparison, error bars are one s.d. estimates of the observations and model predictions in a 12-month window centred at each monthly time step. The standard deviations of the observations are the same as shown in Fig. 1. For the model predictions, the standard deviations take into account variations in model parameters, including the interhemispheric exchange time, the isotopic fractionation, and the isotopic composition of the sources. The slopes of the regression lines and standard deviation estimates are provided in Supplementary Tables 2 and 4.

For this simulation (scenario 2), we assumed that all of the adjustments to the fluxes in both hemispheres (shown in Fig. 2a) were attributed to changes in fossil fuel emissions—with an isotopic signature specific to this source (Supplementary Table 3). The only difference between this scenario and the control run was the inventory of fossil fuel emissions (Supplementary Figs 2 and 3). As expected, this simulation reproduced most of the  $\text{CH}_4$  mixing ratio observations (Supplementary Fig. 3c and d), with decreases in fossil fuel emissions after 1990 (Supplementary Fig. 3a). The decreases in fossil fuel, however, failed to meet

the constraints offered by the measurements of  $\delta^{13}\text{C}\text{-CH}_4$  (Supplementary Fig. 3e). Importantly, the  $\delta^{13}\text{C}$  IHD in this scenario widened during 1989–2005 (Fig. 2b and Supplementary Fig. 3f). This contrasts with the observed  $\delta^{13}\text{C}$  IHD that narrowed during the same time period (Fig. 2b and Supplementary Table 2). In this context, the  $\delta^{13}\text{C}$  IHD observations did not support the hypothesis that decreases in fossil fuel emissions were the main contributor to the  $\text{CH}_4$  slowdown during 1989–2005.

Agriculture, including animal<sup>21</sup> and rice<sup>4</sup> emissions components, is a large term in the contemporary budget<sup>6</sup> and one that has been subject to considerable modification over the past four decades<sup>22,23</sup>. To assess the role of agriculture, we created another scenario (scenario 3) in which we assigned the isotope ratio of the Northern Hemisphere and Southern Hemisphere fluxes needed to match the  $\text{CH}_4$  observations solely to agricultural sources (Supplementary Fig. 4a and b) following the same approach as described above for the fossil fuel scenario. As expected, the agricultural scenario also matched the mixing ratio observations (Supplementary Fig. 4c and d). In contrast with the fossil fuel scenario, however, the  $\delta^{13}\text{C}$  IHD from this run had a positive slope that captured most of the observed trend during 1989–2005 (Fig. 2b and Supplementary Fig. 4f).

We also constructed additional sensitivity and Monte Carlo simulations with our box model examining uncertainties associated with the OH sink, the north–south interhemispheric exchange time for atmospheric mixing, and the isotopic composition of different source terms (as well as potential trends in the isotopic signature of these sources) (Supplementary Tables 2 and 4). Together, these scenarios suggested that our simulation results were robust with respect to our choice of model parameters. Other key uncertainties in our analysis were associated with the representativeness of our reference stations in the Northern and Southern hemispheres, the large variations in  $\text{CH}_4$  and  $\delta^{13}\text{C}\text{-CH}_4$  observed at the beginning of our time series, and the challenges involved in combining stable isotope observations from several laboratories into one long-term time series (comparisons with other available mixing ratio and isotope observations are provided in the Supplementary Information). The mechanisms causing the large variations in the global methane cycle during the early 1990s have not been fully resolved<sup>16</sup> and may influence the long-term trend in the  $\delta^{13}\text{C}\text{-CH}_4$  IHD reported here.

What possible explanations are there for the long-term reductions in microbial sources within the Northern Hemisphere required by the atmospheric isotope observations? Important microbial sources include wetlands, ruminant animals, landfills and rice agriculture. We summarize below evidence that decreasing emissions from rice agriculture probably accounted for some of the observed source reductions in the Northern Hemisphere, using a biogeochemical model to synthesize information from country-level agricultural statistics and recent field studies. Improved management of landfills also may have contributed to Northern Hemisphere source reductions<sup>23</sup>. For ruminant animals and wetlands, however, key processes regulating these sources have not changed in a way that is consistent with the long-term decreases in emissions needed to explain the atmospheric observations<sup>21–25</sup>.

Reductions in rice agriculture emissions have occurred primarily from land use intensification rather than changes in the area of rice production. Statistics compiled by the International Rice Research Institute<sup>26</sup> show that the world's rough rice (that is, unprocessed paddy rice) areas did not change by a substantial amount between 1980 and 2005 (Fig. 3a). Considering rice production areas alone, trends over the past several decades are consistent with a stabilization of fluxes, but not the overall reduction needed to explain the  $\text{CH}_4$  mixing ratio and isotope observations presented here.

Accumulating evidence suggests, however, that application of chemical fertilizer<sup>9</sup> and more efficient water use<sup>10</sup> substantially reduces  $\text{CH}_4$  emissions per unit of area of rice production.  $\text{CH}_4$  fluxes in rice fields are strongly regulated by levels of organic fertilizer input<sup>27</sup>. Chemical fertilizer application in China and India increased substantially from 1970 to 2005 (Fig. 3c). The rapid rise in chemical fertilizer

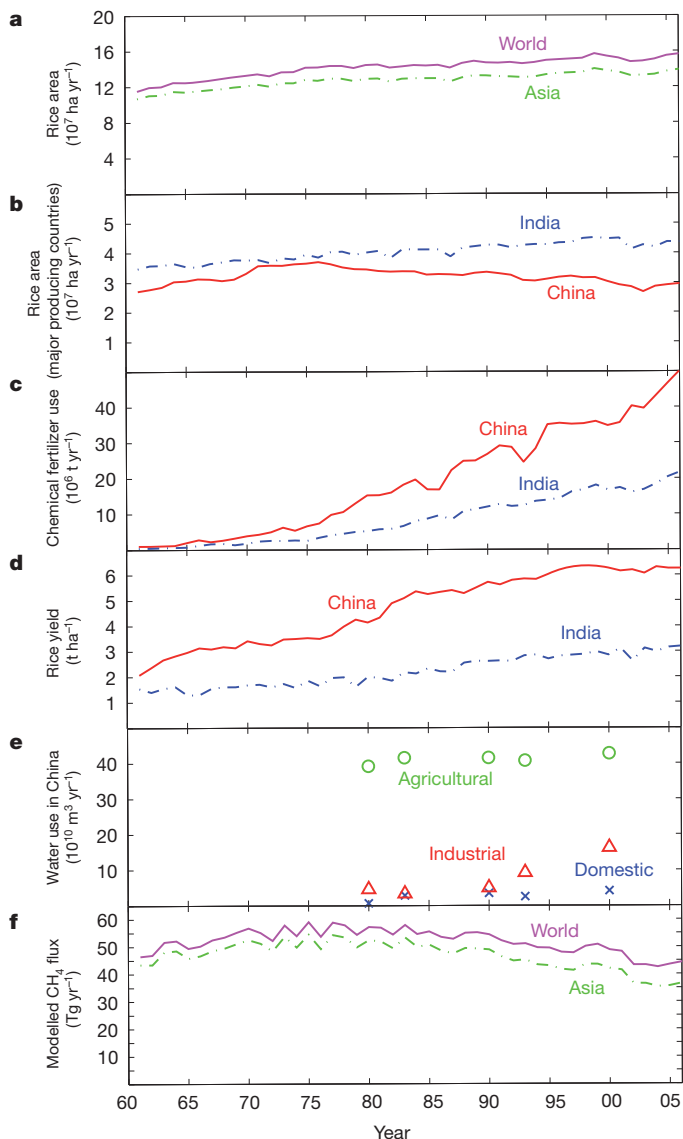


**Figure 3 | Evidence for intensification of rice agriculture in Asia.** The total world area under rice production has not substantially changed since the late 1970s and is dominated by production in Asian countries (a). The two largest rice-producing countries during 1960–2005 were China and India (b). The use of chemical fertilizer in both countries, especially China, increased substantially during the same time period (c). The increase in rice yield (d) was consistent with rapid increases in chemical fertilizer application and implied a weakening dependence on organic fertilizer, which is both labour-intensive and a primary substrate for  $\text{CH}_4$  production. Growing industrial water demand after the 1980s reduced the percentage of water withdrawals available for agriculture in China (e) and may be one factor contributing to new mid-season drainage practices. After the early 1980s, decreases in global  $\text{CH}_4$  emissions from rice agriculture were predicted to occur on the basis of an analysis from a biogeochemical process model driven by climate, rice area, fertilizer and water management information (f).

use is consistent with concurrent increases in rice yield (Fig. 3d) and reductions in organic amendments that are more labour-intensive<sup>9</sup>. Other studies have shown that changing the water management of rice paddies can reduce  $\text{CH}_4$  emissions by about 10–80% (refs 10, 11 and 27). At the country level, increasing urban and industrial demands for water have increased since 1980 and have limited the water available for agriculture<sup>28</sup> (Fig. 3e).

To assess the magnitude of emissions changes associated with rice agriculture during 1960–2005, we modified an empirically based biogeochemical process model<sup>29,30</sup> to include fertilizer application and



water management impacts on rice yield and methane fluxes (see Supplementary Information). Using this model, which is driven by climate, production area statistics, fertilizer inputs and management information, we estimated that the Northern Hemisphere rice emissions reached a maximum in the early 1980s and decreased by about  $15.5 \pm 1.9 \text{ Tg yr}^{-1}$  between 1984 and 2005 (Fig. 3f). The decreasing trend in emissions explained approximately half ( $51 \pm 18\%$ ) of the observed trend inferred from the atmospheric  $\text{CH}_4$  measurements (Fig. 2a).

Here we found that the increasing enrichment of  $\delta^{13}\text{C}$  in the Northern Hemisphere and a narrowing of the  $\delta^{13}\text{C}$  IHD provided new information about the causes of the  $\text{CH}_4$  slowdown between 1989 and 2005. Model simulations indicated that decreases in Northern Hemisphere microbial sources had an isotopic signature consistent with the observed atmospheric changes. Although changes in atmospheric OH levels and fossil fuel emissions probably contributed to some of the variability during this period<sup>5,7,8</sup>, the trends in the  $\delta^{13}\text{C}$  IHD presented here excluded these changes as the most important contributors to the long-term  $\text{CH}_4$  slowdown. Changes in management of rice agriculture probably contributed to some of the observed decline in Northern Hemisphere emissions, on the basis of estimates from a biogeochemical model. Evaluating the net impact of these management changes on climate requires careful consideration of other greenhouse gas fluxes, including production of  $\text{N}_2\text{O}$  (see, for example, ref. 11). The future trajectory of  $\text{CH}_4$  remains difficult to predict, with recent increases after 2006 potentially attributable to emissions from Northern Hemisphere wetlands<sup>25</sup> and biomass burning in the tropics<sup>3</sup>. Our work demonstrates the importance of considering changing agricultural practices in addition to climate effects on natural sources as key drivers of future atmospheric  $\text{CH}_4$  levels.

## METHODS SUMMARY

To quantify the IHDs of  $\text{CH}_4$ ,  $\delta^{13}\text{C}\text{-CH}_4$  and  $\delta\text{D}\text{-CH}_4$ , we constructed a long-term time series in each hemisphere (at  $40^\circ\text{N}$  and  $41^\circ\text{S}$ ) by using measurements from the UCI, NIWA and SIL networks<sup>2,15–17</sup>. These data were selected because they possessed multi-year  $\delta^{13}\text{C}$  and  $\delta\text{D}$  measurements of atmospheric  $\text{CH}_4$  required in our analysis for constraining  $\text{CH}_4$  source and sink processes. We then used a two-box atmospheric model<sup>18</sup> that included information about  $\text{CH}_4$  source and sink processes (and their impacts on isotopic fractionation) to examine various hypotheses formulated to explain the overall decline in the  $\text{CH}_4$  growth rate. We forced the model using emissions inventories (see, for example, ref. 22) for anthropogenic emissions from 1700 to 1980, and in our control simulation these emissions were held constant thereafter (through 2005). The model included changes in soil and animal  $\text{CH}_4$  source isotopic composition over the past two centuries induced by changes in  $\delta^{13}\text{C}\text{-CO}_2$ . Finally, to evaluate changes in rice agricultural sources over the past few decades, we used an empirical process-based biogeochemical model with parameterizations derived from field measurements<sup>29,30</sup>. We forced the biogeochemical model with time series of rough rice area and fertilizer application rates using data from the International Rice Research Institute<sup>26</sup>. Details of the sampling and measuring procedure, comparisons of our measurements with observations from other networks, analysis methods, and modelling approaches are described in the Supplementary Information. The main constraints offered by the observed mixing and isotopic ratios described above are summarized in a schematic figure (Supplementary Fig. 5).

Received 3 March 2010; accepted 18 May 2011.

1. Dlugokencky, E. J., Masarie, K. A., Lang, P. M. & Tans, P. P. Continuing decline in the growth rate of the atmospheric methane burden. *Nature* **393**, 447–450 (1998).
2. Simpson, I. J., Rowland, F. S., Meinardi, S. & Blake, D. R. Influence of biomass burning during recent fluctuations in the slow growth of global tropospheric methane. *Geophys. Res. Lett.* **33**, L22808 (2006).
3. Dlugokencky, E. J. *et al.* Observational constraints on recent increases in the atmospheric  $\text{CH}_4$  burden. *Geophys. Res. Lett.* **36**, L18803 (2009).
4. Khalil, M. A. K. & Shearer, M. J. in *Atmospheric Methane: its Role in the Global Environment* (ed. Khalil, M. A. K.) 98–111 (Springer, 2000).
5. Bousquet, P. *et al.* Contribution of anthropogenic and natural sources to atmospheric methane variability. *Nature* **443**, 439–443 (2006).
6. Forster, P. *et al.* in *Climate Change 2007: The Physical Science Basis* (eds Solomon, S. D. *et al.*) 129–234 (Cambridge Univ. Press, 2007).

7. Fiore, A. M., Horowitz, L. W., Dlugokencky, E. J. & West, J. J. Impact of meteorology and emissions on methane trends, 1990–2004. *Geophys. Res. Lett.* **33**, L12809 (2006).
8. Dlugokencky, E. J. *et al.* Atmospheric methane levels off: temporary pause or a new steady-state? *Geophys. Res. Lett.* **30**, 1992, doi:10.1029/2003GL018126 (2003).
9. Denier van der Gon, H. Changes in  $\text{CH}_4$  emission from rice fields from 1960 to 1990s. 2. The declining use of organic inputs in rice farming. *Glob. Biogeochem. Cycles* **13**, 1053–1062 (1999).
10. Li, C. S. *et al.* Reduced methane emissions from large-scale changes in water management of China's rice paddies during 1980–2000. *Geophys. Res. Lett.* **29**, 1972, doi:10.1029/2002GL015370 (2002).
11. Frohling, S., Li, C. S., Braswell, R. & Fuglestedt, J. Short- and long-term greenhouse gas and radiative forcing impacts of changing water management in Asian rice paddies. *Glob. Change Biol.* **10**, 1180–1196 (2004).
12. Worthy, D. E. J. *et al.* Decreasing anthropogenic methane emissions in Europe and Siberia inferred from continuous carbon dioxide and methane observations at Alert, Canada. *J. Geophys. Res.* **114**, D10301, doi:10.1029/2008JD011239 (2009).
13. Cicerone, R. J. & Oremland, R. S. Biogeochemical aspects of atmospheric methane. *Glob. Biogeochem. Cycles* **2**, 299–327 (1988).
14. Lassey, K. R., Etheridge, D. M., Lowe, D. C., Smith, A. M. & Ferretti, D. F. Centennial evolution of the atmospheric methane budget: what do the carbon isotopes tell us? *Atmos. Chem. Phys.* **7**, 2119–2139 (2007).
15. Tyler, S. C., Rice, A. L. & Ajie, H. O. Stable isotope ratios in atmospheric  $\text{CH}_4$ : implications for seasonal sources and sinks. *J. Geophys. Res.* **112**, D03303 (2007).
16. Lowe, D. C., Manning, M. R., Brailsford, G. W. & Bromley, A. M. The 1991–1992 atmospheric methane anomaly: Southern Hemisphere  $^{13}\text{C}$  decrease and growth rate fluctuations. *Geophys. Res. Lett.* **24**, 857–860 (1997).
17. Quay, P. *et al.* The isotopic composition of atmospheric methane. *Glob. Biogeochem. Cycles* **13**, 445–461 (1999).
18. Tans, P. P. A note on isotopic ratios and the global atmospheric methane budget. *Glob. Biogeochem. Cycles* **11**, 77–81 (1997).
19. Etheridge, D. M., Steele, L. P., Francey, R. J. & Langenfelds, R. L. Atmospheric methane between 1000 AD and present: evidence of anthropogenic emissions and climatic variability. *J. Geophys. Res.* **103**, 15979–15993 (1998).
20. Ferretti, D. F. *et al.* Unexpected changes to the global methane budget over the past 2000 years. *Science* **309**, 1714–1717 (2005).
21. Lassey, K. R. Livestock methane emission: from the individual grazing animal through national inventories to the global methane cycle. *Agric. For. Meteorol.* **142**, 120–132 (2007).
22. van Aardenne, J. A., Dentener, F. J., Olivier, J. G. J., Goldewijk, C. G. M. K. & Lelieveld, J. A  $1^\circ \times 1^\circ$  resolution data set of historical anthropogenic trace gas emissions for the period 1890–1990. *Glob. Biogeochem. Cycles* **15**, 909–928 (2001).
23. *Global Anthropogenic Non-CO<sub>2</sub> Greenhouse Gas Emissions: 1990–2020* (<http://www.epa.gov/climatechange/economics/downloads/GlobalAnthroEmissionsReport.pdf>) (United States Environmental Protection Agency, 2006).
24. Zhuang, Q. *et al.* Methane fluxes between terrestrial ecosystems and the atmosphere at northern high latitudes during the past century: a retrospective analysis with a process-based biogeochemistry model. *Glob. Biogeochem. Cycles* **18**, GB3010 (2004).
25. Bloom, A. A., Palmer, P. I., Fraser, A., Reay, D. & Frankenberg, C. Large-scale controls of methanogenesis inferred from methane and gravity spaceborne data. *Science* **327**, 322–325 (2010).
26. *World Rice Statistics* (<http://irri.org/world-rice-statistics>) (International Rice Research Institute, 2008; accessed 22 September 2008).
27. Wassmann, R. *et al.* Characterization of methane emissions from rice fields in Asia. III. Mitigation options and future research needs. *Nutr. Cycl. Agroecosyst.* **58**, 23–36 (2000).
28. *Water Use Statistics* (<http://www.fao.org/nr/water/aquastat/main/index.stm>) (Food and Agriculture Organization of the United Nations, 2008; accessed 22 September 2008).
29. Huang, Y., Sass, R. L. & Fisher, F. M. A semi-empirical model of methane emission from flooded rice paddy soils. *Glob. Change Biol.* **4**, 247–268 (1998).
30. Kai, F. M., Tyler, S. C. & Randerson, J. T. Modeling methane emissions from rice agriculture in China during 1961–2007. *J. Integr. Env. Sci.* **7**, 49–60 (2010).

Supplementary Information is linked to the online version of the paper at [www.nature.com/nature](http://www.nature.com/nature).

**Acknowledgements** We thank the many researchers associated with the laboratories referred to as NOAA, NIWA, UW and UCI who took part in collecting and measuring many thousands of air samples over the years. We also thank P. Bousquet for detailed comments on earlier drafts that improved the manuscript. This work has been funded by NASA grants to S.C.T. (NGT5-30409) and J.T.R. (NNX08AF64G), NSF grants to S.C.T. (ATM 9871077) and J.T.R. (ATM-0628637 and AGS-1021776), and additional support from the W. M. Keck Foundation.

**Author Contributions** S.C.T., F.M.K. and D.R.B. carried out  $\text{CH}_4$ ,  $\delta^{13}\text{C}\text{-CH}_4$  and  $\delta\text{D}\text{-CH}_4$  measurements. F.M.K., S.C.T. and J.T.R. designed the study. F.M.K. conducted data analysis and performed the model simulations. F.M.K., S.C.T. and J.T.R. wrote the paper. All authors discussed the results and commented on the manuscript.

**Author Information** Reprints and permissions information is available at [www.nature.com/reprints](http://www.nature.com/reprints). The authors declare no competing financial interests. Readers are welcome to comment on the online version of this article at [www.nature.com/nature](http://www.nature.com/nature). Correspondence and requests for materials should be addressed to F.M.K. ([fmkai@smart.mit.edu](mailto:fmkai@smart.mit.edu)).